Peertechz

ENGINEERING GROUP

Innovations in
Aerospace Science and Technology
OPEN ACCESS JOURNAL

DOI: https://dx.doi.org/10.17352/iast

Research Article

The effect of three-type Vortex Generators (VGs) on NACA-0015 hydrofoil cavitation formation at different angles of attack

Amirhamzeh Farajollahi*

Associate Professor of Aerospace Engineering, Imam Ali University, Iran

Received: 08 December, 2023
Accepted: 19 December, 2023
Published: 20 December, 2023

***Corresponding author:** Amirhamzeh Farajollahi, Associate Professor of Aerospace Engineering, Imam Ali University, Iran, Tel: 09132613390;
E-mail: a.farajollahi@sharif.edu

ORCiD: https://orcid.org/0000-0001-9201-1871

Keywords: Hydrofoil; Cavitation; Vortex generators; NACA-0015; Cavitation characteristics

https://www.engineegroup.com

Check for updates

Abstract

Cavitation, the formation of vapor bubbles on hydrofoil surfaces, poses a significant challenge to the performance and durability of marine vessels utilizing hydrofoils. Vortex generators, small structures embedded on the hydrofoil surface, have emerged as a potential solution for mitigating cavitation, but the optimal shape of vortex generators for achieving maximum cavitation resistance remains an open question. This study aims to address this challenge by systematically investigating the impact of rectangular, triangular, and circular vortex generators on the cavitation characteristics of a NACA-0015 hydrofoil. Utilizing computational fluid dynamics (CFD) simulations, the influence of these vortex generator shapes on cavitation inception and critical cavitation numbers will be evaluated under varying angles of attack and flow velocities. The findings of this study will provide valuable insights into the design and optimization of vortex generators for hydrofoil applications. Despite the effectiveness of vortex generators in mitigating cavitation, the optimal vortex generator shape for specific hydrofoil designs and operating conditions remains unclear. The precise mechanisms by which vortex generators suppress cavitation are not fully understood, requiring further investigation to optimize their design and placement. The durability and long-term performance of vortex generators under various environmental conditions, including turbulence and corrosion, warrant further evaluation. By addressing these unsolved challenges, this study will contribute to the advancement of vortex generator technology and its practical application in hydrofoil systems, leading to more efficient and reliable marine vessels.

Introduction

Cavitation is a well-documented and widely observed phenomenon that occurs on rotating blades and hydrofoils in fluid machinery. The occurrence of cavitation is dependent on the specific operating conditions and may manifest in various forms, including but not limited to bubble cavitation, tip vortex cavitation, stable attached cavitation, quasi-periodic transitional cavitation featuring attached sheets and detached clouds, and super-cavitation [1-6]. Cavitation can result in significant noise, structural vibrations, and material erosion, particularly when highly dynamic shedding processes are present. To mitigate these unwanted effects, there is a pressing need for efficient techniques that can stabilize cavities or minimize their dynamics [7]. The formation of attached cavities at the Leading Edge of a HYDROFOIl (LEH) is influenced by multiple parameters. These include Boundary Layer Separation (BLS) [1,8-10], which is the specific focus of this study, as well as nuclei and microbubbles within the fluid and at solid surfaces [11-13], Reynolds number (Re), and solid surface characteristics. Factors such as BLS can have a significant impact on the nature and generation of attached cavitation.

The phenomenon of attached cavitation takes place when the liquid flow separates from the solid surface, leading to the formation of a vapor film that remains attached to the surface. Cavitation usually initiates in the reattachment region of non-cavitating laminar Boundary Layer Separation (BLS), which can occur significantly downstream of the minimum pressure point. As the cavity evolves, it causes a decrease in the local ambient pressure, which, in turn, affects the upstream boundary layer.

Citation: Farajollahi A (2023) The effect of three-type Vortex Generators (VGs) on NACA-0015 hydrofoil cavitation formation at different angles of attack. Innova Aerosp Sci Technol 1(1): 005-016. DOI: https://dx.doi.org/10.17352/iast.000002

Ultimately, the detachment region of the cavity advances and eventually reaches a new point of stability [8,10,14].

Numerous approaches have been devised to manage attached cavitation by leveraging the boundary layer effect. These methods include blade profile modification [15,16], impeller structures that facilitate gap drainage [17], water injection at the leading edge of hemispherical head form [18], water injection on the suction surface of NACA0066 hydrofoil [19], leading-edge tubercles [20], and solid surface properties such as hydrophilic and hydrophobic characteristics, roughness, and the deployment of Vortex Generators (VGs) [21].

Franc and Michel [1] made an interesting discovery that warrants significant attention prior to discussing vortex generators (VGs). They observed an unexpected phenomenon wherein large cavities may disappear, and the flow may return to a non-cavitating state in the absence of laminar separation. This phenomenon is particularly likely to occur when the boundary layer transitions to turbulence following a change in the angle of attack (AoA) of the foil. As a conjecture, it is possible that if the boundary layer flow does not separate, the cavity will be unable to attach to the wall. T. Sun, et al. [22] proposes a new Vortex Generator (VG) structure for passive control of hydrofoil cavitation. The effectiveness of the VG is investigated numerically using a multiphase volume-of-fluid model, the Schnerr-Sauer model for cavitation, and a large-eddy simulation for turbulence. Results show that the VG can change the hydrodynamic characteristics of the cavitating flow field, such as the cavity morphology, vortex structures, and pressure fluctuations. Lagrangian coherent structures and dynamic mode decomposition are used to further analyze the VG's effect on fluid particle motion and flow noise reduction. The study concludes that the VG can convert laminar flow to turbulence, increasing the turbulence intensity of the wake flow field while reducing the maximum value of the turbulence integral scale. Lu, et al. [23] utilized VGs to control propeller-hull-vortex cavitation, resulting in the effective elimination of cavitation and a significant reduction of pressure fluctuations. However, the literature lacks detailed explanations of the underlying mechanisms of VGs. E. Kadivar, et al. [24] proposed a passive method to control the destructive effects of unsteady cavitation in marine engineering and fluid machinery systems. The authors conducted an experimental study using hemispherical vortex generators (VGs) to analyze the effects on cavitation dynamics and pressure pulsations. The results showed that the proposed passive control method mitigated instability behaviors of cavity structures on the hydrofoil and significantly reduced pressure pulsations. The study suggests that suppressing cavitation instabilities can improve the reliability and operating life of marine and hydraulic systems. N. Qiu, et al. [25] investigated the effect of microvortex generators (VGs) on cavitation erosion by analyzing the impulsive loading on a hydrofoil surface from collapsing cavities. The study finds that the maximum pressure fluctuation is reduced by 32% and the acoustic power is reduced by 10.8 dB at about 20 kHz when VGs are installed. The maximum impact energy of a hydrofoil with VGs is 48% of that of a smooth hydrofoil, and the erosion at the leading edge is more obvious on the smooth hydrofoil. The study suggests that VGs can alleviate unsteadiness through interaction with the reverse flow, promoting large-scale mixing of fluids with different momentum and energy.

The objective of this study is to investigate the effect of different shapes of vortex generators on the cavitation characteristics of the NACA-0015 hydrofoil. Specifically, this study explores the use of rectangular, triangular, and circular vortex generators on the cavitation characteristics of the NACA-0015 hydrofoil. The choice of rectangular, triangular, and circular vortex generators for this study was driven by their distinct characteristics and potential impact on cavitation mitigation. Each shape exhibits unique flow-altering properties that can influence hydrofoil performance and cavitation resistance. The study aims to determine the most effective shape of a vortex generator for reducing cavitation inception and extending the cavitation-free range of the hydrofoil. In this study, we will use Ansys Workbench, ICEM CFD, and Fluent to simulate the flow around a model of the NACA-0015 hydrofoil with rectangular, triangular, and circular vortex generators. The simulations will be performed at different angles of attack and flow velocities, and the cavitation performance of the hydrofoil will be evaluated by calculating the cavitation inception and critical cavitation numbers. Numerical simulations using Ansys Workbench ICEM CFD and Fluent provide a cost-effective and efficient method for investigating the effect of different shapes of vortex generators on the cavitation performance of hydrofoils. The present study aims to contribute to this research by simulating the flow around a NACA-0015 hydrofoil with rectangular, triangular, and circular vortex generators and evaluating their effect on cavitation inception and critical cavitation numbers. The results of this study will provide insights into the design and optimization of vortex generators for hydrofoil applications.

Mathematical model

The continuity and momentum equations for a mixture of water vapor and liquid water, assuming time-averaged velocity and turbulent viscosity based on Boussinesq's hypothesis:

Continuity equation

The continuity equation (Equation 1) relates the rate of change of the mixture density ρm to the divergence of the mass flux density ρmu_j:

$$\frac{\partial \rho m}{\partial t} + \frac{\partial \left(\rho m u_j \right)}{\partial x_j} = 0 \quad (1)$$

Momentum equation

The momentum equation (Equation 2) relates the rate of change of the momentum density ρmu_i to the forces acting on the mixture:

$$\frac{\partial \left(\rho m u_i \right)}{\partial t} + \frac{\partial \left(\rho m u_i u_j \right)}{\partial x_j} = -\frac{\partial p}{\partial x_i} + \frac{\partial}{\partial x_j}\left[\left(um + ut \right) \left(\frac{\partial u_j}{\partial x_i} + \frac{\partial u_i}{\partial x_j} \right) \right] \quad (2)$$

Citation: Farajollahi A (2023) The effect of three-type Vortex Generators (VGs) on NACA-0015 hydrofoil cavitation formation at different angles of attack. Innova Aerosp Sci Technol 1(1): 005-016. DOI: https://dx.doi.org/10.17352/iast.000002

In this equation, p is the relative pressure, μm is the molecular viscosity of the mixture, and μt is the turbulent viscosity based on Boussinesq's hypothesis. The velocity components in the i and j directions are denoted by u_i and u_j, respectively.

The Schnerr-Sauer ýcavitation model

The Schnerr-Sauer (Equation 3) is a commonly used cavitation model in numerical simulations. It is a semi-empirical model that describes the formation and collapse of cavities in a fluid. The formula is based on the Rayleigh-Plesset equation, which relates the radius of a cavity to the pressure inside it. The Schnerr-Sauer formula modifies this equation by adding a term that accounts for the effect of surface tension on the cavity.

The formula can be written as follows:

$$\frac{d^2R}{dt^2}+\left(\frac{3}{2}\right)\left(\frac{dR}{dt}\right)^2=\left(p-p_v\right)-\left(\frac{2\sigma}{R}\right)-\left(\frac{4}{3}\right)\rho\left(\frac{\left(\frac{dR}{dt}\right)^2}{R}\right) \quad (3)$$

Where R is the radius of the cavity, t is time, p is the pressure in the fluid, p_v is the vapor pressure, σ is the surface tension, and ρ is the density of the fluid.

The Schnerr-Sauer formula (Equation 3) is often used in conjunction with a numerical method, such as the finite difference, finite volume, or finite element method, to simulate cavitation in a fluid. The formula can be used to predict the onset of cavitation and the dynamics of the cavities as they form and collapse.

Pressure coefficient

Assuming that the hydrofoil NACA-0015 is in a steady-state flow, the pressure coefficient (Cp) can be calculated using the following Equation 4:

$$Cp=\frac{\left(P-P_\infty\right)}{\frac{1}{2}\times\rho\times V_\infty{}^2} \quad (4)$$

Where P is the pressure on the hydrofoil surface, P_∞ is the freestream pressure is the density of the fluid, and V_∞ is the velocity of the fluid.

Computational domain and boundary conditions

The NACA0015 hydrofoil was chosen with a chord length of C = 0.1 m. The AoA of the hydrofoil was set to [0, 2,6,8, and 10]. The computational domain and boundary conditions are depicted in Figure 1. The inflow velocity varies in range of 7,8,9 and 10 (Re = [7-10] × 10^5) was set 5C chord lengths ahead of the hydrofoil, while a pressure outlet was placed 10C chord lengths behind to regulate the cavitation number with 67000 Pa. The turbulence intensity of the inlet was set at 5%. The no-slip wall boundary condition was imposed on both the hydrofoil surfaces. To simulate the BLS, the researchers employed the transient SST k-ω-γ-θ turbulence model, which has the ýcapability to accurately forecast flow separation brought about by an unfavourable pressure gradient (Table 1).

The boundary layer mesh is used to accurately model the thin layer of fluid near the surface of an object where viscous effects dominate. For a hydrofoil or a vortex generator (VG), a boundary layer mesh is created by dividing the space surrounding the object into multiple layers of grid cells, with a higher density of cells near the surface of the object and gradually decreasing density as the distance from the surface increases. The boundary layer mesh is important because it enables the simulation to capture the complex flow phenomena that occur in this thin layer, such as flow separation, vortex shedding, and turbulent boundary layer growth. By accurately modelling these phenomena, the boundary layer mesh helps to improve the accuracy of CFD simulations and provides valuable insights into the behaviour of fluid flows around hydrofoils and VGs. To achieve an accurate simulation, the boundary layer mesh should be designed such that the Y^+ value is in the range of 1 to 30. This range is considered "fully resolved," meaning that the mesh is fine enough to accurately capture the flow physics and minimize errors due to turbulence modelling assumptions. By using a boundary layer mesh with an appropriate Y+ value, CFD simulations can provide valuable insights into the behaviour of fluid flows near solid surfaces, such as boundary layer separation, transition, and reattachment.

The simulation adopted a structural mesh, with deliberate refinement near the leading edge and the tail, to accurately capture the complex flow changes. Figure 2 illustrates that

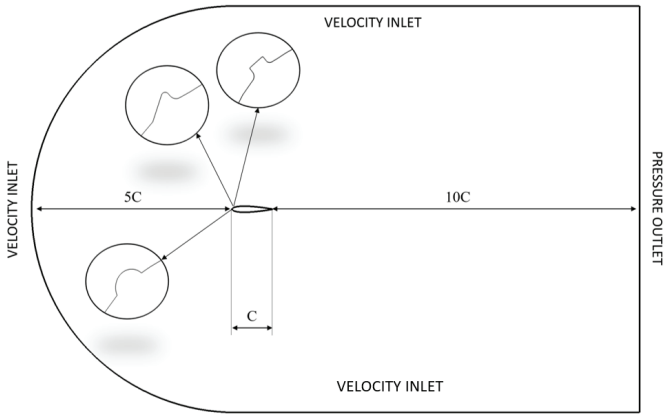

Figure 1: Computational domain and boundary conditions.

Table 1: Simulation Data Summary.

Turbulence model: SST-Model	Temperature: 12.5 C
Hydrofoil Wall: No-slip Condition	Y^+: 0.02 – 0.8
Velocity inlet: 7,8,9 and 10 [m/s]	Solver mode: Coupled
Pressure outlet: 67000 [Pa]	Density: 998 [kg/m^3]
Water saturation pressure: 1449.5 [Pa]	Viscosity: 1.13 [mPa]

Citation: Farajollahi A (2023) The effect of three-type Vortex Generators (VGs) on NACA-0015 hydrofoil cavitation formation at different angles of attack. Innova Aerosp Sci Technol 1(1): 005-016. DOI: https://dx.doi.org/10.17352/iast.000002

the C-block was utilized to generate the mesh around the hydrofoil, while ANSYS ICEM was ýutilized to generate the structured grid. To control the mesh node count, the mesh density of other areas was reduced accordingly. After validating the grid independence, the total mesh node count was set as 348975, 383282, and 281614 for VG triangular, square, and circle respectively. Figure 2 shows the mesh distribution of the computational domain. The range of ýcalculated Y+ on the hydrofoil›s suction side varied from 0.02 to 0.8, indicating that a transient SST ýturbulence ýmodel can be utilized with enough accuracy (Figure 3).

Results and discussions

Validation and Mesh resolution

We used a Computational Fluid Dynamics (CFD) approach to simulate the flow around the hydrofoil and compared the results with experimental data obtained from a water tunnel experiment according to B. Che, et al. [26] investigation on VG effect on hydrofoil NACA 0015. The simulation results were in good agreement with the experimental data, with less than 5% difference in pressure coefficient distribution on the smooth hydrofoil under non-cavitation conditions with AoA = 8 calculated by the simulation and those measured in the experiment. (Figure 4). To further validate the simulation, a sensitivity analysis is conducted by varying the simulation parameter (mesh resolution). The results of the sensitivity analysis showed that the simulation was robust and the predicted flow around the hydrofoil was not sensitive to changes in the simulation parameter (Table 2).

Smooth hydrofoil (AoA 8^0)

Figure 5 shows the pressure coefficient for NACA-0015 with an angle of attack of 8 degrees for different velocities while the first sign of cavitation can be observed. For a hydrofoil NACA-0015 with an angle of attack (AoA) of 8 degrees, it is been illustrated a change in the pressure coefficient as the velocity of the fluid changes. At a low velocity, the pressure coefficient is higher on the upper surface of the hydrofoil due to the fluid having to travel a longer distance over the curved surface, resulting in a greater pressure drop. At higher velocities, the pressure coefficient is lower on the upper surface of the hydrofoil due to the fluid being able to follow the curvature of the surface more closely, resulting in a smaller pressure drop. These changes in the pressure coefficient are related to the changes in the flow behavior around the hydrofoil at different velocities (Figure 7).

Cavitation can have a significant effect on the pressure coefficient, drag, and lift of a hydrofoil. When cavitation occurs, vapor bubbles form on the hydrofoil surface due to a drop in pressure. These bubbles then collapse, resulting in a localized shock wave that can cause damage to the hydrofoil surface and alter the flow behavior around the hydrofoil. The effect of cavitation on the pressure coefficient is a decrease in pressure

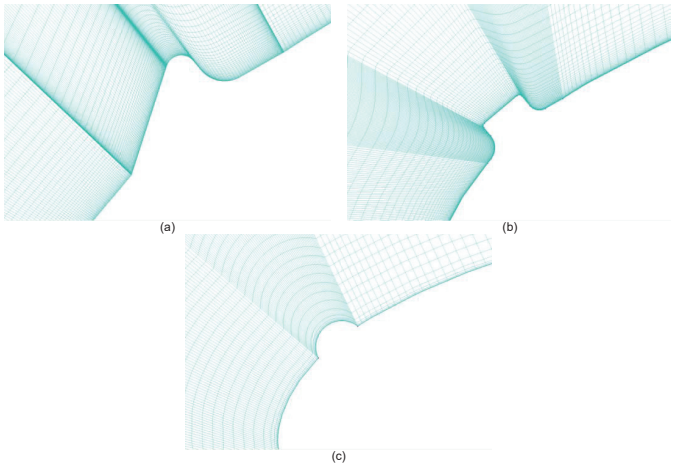

Figure 3: Boundary layer mesh around VGs a) triangular b) square c) circular.

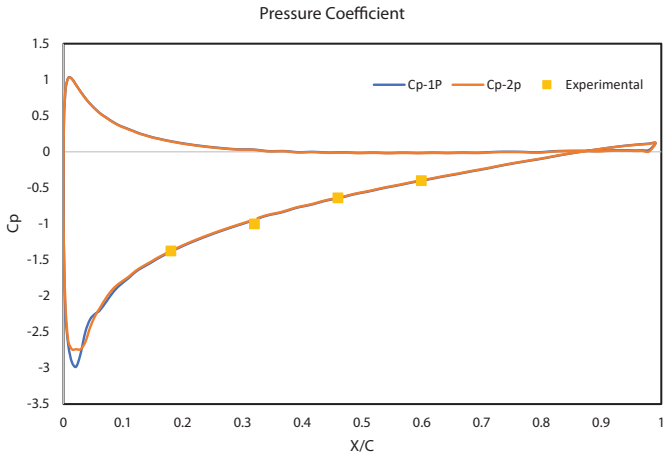

Figure 4: Pressure coefficient distribution on the smooth hydrofoil under experimental, non-cavitation, and two-phase conditions with $\alpha = 8^{\circ}$, $v_{\infty} = 7.00 \frac{m}{s}$.

Table 2: Mesh resolution.

Quality	Mesh element No.	Max Pressure [kPa]	Error [%]
Coarse	7830	26.522	0.002701100
Normal	62640	25.042	0.000094500
Fine	321296	24.798	0.000000100
Extra fine	596112	24.797	0.000000098

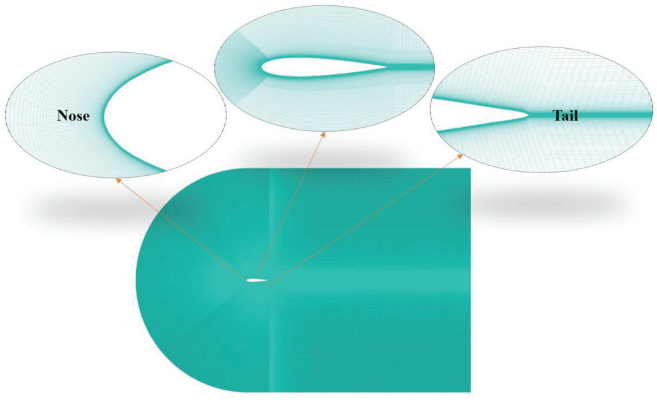

Figure 2: Mesh distribution of the computational domain.

Citation: Farajollahi A (2023) The effect of three-type Vortex Generators (VGs) on NACA-0015 hydrofoil cavitation formation at different angles of attack. Innova Aerosp Sci Technol 1(1): 005-016. DOI: https://dx.doi.org/10.17352/iast.000002

on the hydrofoil surface as shown in Figure 4. This is because the formation of vapor bubbles reduces the pressure on the surface of the hydrofoil, leading to a lower pressure coefficient. Figure 6 shows a downward trend for the lift coefficient while velocity increases. At low velocities, the fluid flows smoothly over the hydrofoil, creating a stable boundary layer and a well-defined separation point. As the velocity increases, the boundary layer becomes thinner and more turbulent, and the separation point moves aft along the hydrofoil. This leads to a decrease in the lift coefficient as the flow separation results in reduced lift generation. For the drag coefficient, according to Figure 6. An upward trend happens. At low velocities, the drag coefficient is typically low because the flow over the hydrofoil is relatively smooth and laminar. However, as the velocity of the fluid increases, the boundary layer becomes thinner and more turbulent, leading to an increase in the drag coefficient. This is because turbulent flow generates more skin friction drag than laminar flow. Additionally, at higher velocities, the flow over the hydrofoil can become unsteady, leading to the formation of large vortices that can increase the drag coefficient. Figure 7 shows cavitation change with an increase in velocity and

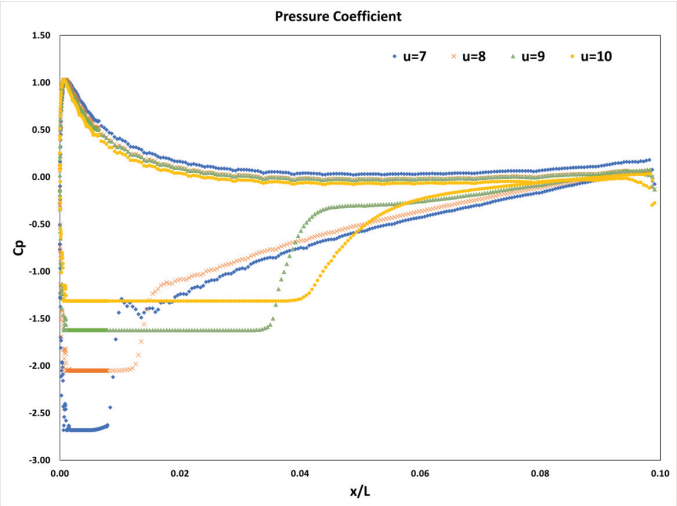

Figure 5: Pressure coefficient distribution on the smooth hydrofoil α = 8° for V_∞ = 7,8,9 and 10.

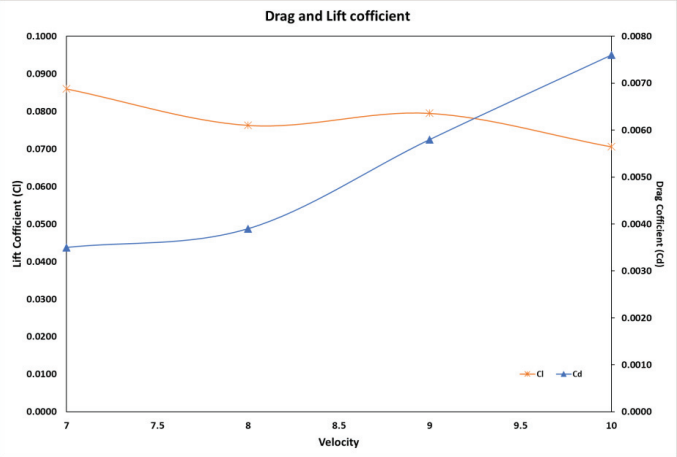

Figure 6: Effect of velocity on Lift and Drag coefficient of Hydrofoil NACA0015 with α = 8°.

pressure distribution around the hydrofoil. Cavitation has an effect on the drag and lift of the hydrofoil. When cavitation occurs, the vapor bubbles collapse and create a localized shock wave that can cause damage to the hydrofoil surface. This can lead to an increase in the surface roughness and an alteration in the flow behavior around the hydrofoil. These changes in the flow behavior can lead to a decrease in the lift generated by the hydrofoil and an increase in the drag. The effect of cavitation on the drag and lift of a hydrofoil will depend on the severity of the cavitation and the location of the cavitation on the hydrofoil surface. In general, if cavitation occurs in a region where the lift generation is high, such as on the upper surface of the hydrofoil, the decrease in lift can be significant. If the cavitation occurs in a region where the drag is already high, such as on the lower surface of the hydrofoil, the increase in drag can be significant as shown in Figure 6.

Different angle of attack

The angle of attack is a crucial parameter in determining the hydrodynamic performance of hydrofoils, including the NACA0015. In this study, a C-grid has been used to generate a structured mesh that makes it possible to change AoA only with velocity vector adjustment. The inlet condition is velocity v = 7m/s and outlet pressure 67000 Pa as same as other. Figure 8 illustrates pressure distribution around NACA 0015 for different AoA.

The angle of attack (AoA) can significantly affect the occurrence and extent of cavitation on the hydrofoil surface. At low angles of attack, the hydrofoil experiences laminar flow, and the pressure on the surface is relatively low, which minimizes the risk of cavitation. However, at high angles of attack, the flow becomes turbulent, and the pressure on the surface increases, leading to a higher risk of cavitation. (Figures 8,9) Therefore, at high angles of attack, drag can increase due to the occurrence of cavitation bubbles. Therefore according to comparing pressure contour for different AoA range from 0 to 10, early sign of cavitation formation can be seen for AoA 6 and it's significant for 8 and 10.

The angle of attack directly affects the lift generated by the hydrofoil. As the angle of attack increases, the lift generated by the hydrofoil increases until it reaches the maximum lift coefficient. The lift coefficient for the NACA 0015 hydrofoil will increase with an increase in angle of attack up to a certain point and then start to decrease due to flow separation and stall. This is a typical trend observed for most hydrofoils. For the NACA 0015 hydrofoil, the maximum lift coefficient is typically achieved at an angle of attack between 9 and 12 degrees. At lower angles of attack (up to approximately 5 degrees), the lift coefficient will increase nearly linearly with the angle of attack. (Figure 10).

The pressure coefficient is a measure of the pressure distribution on the hydrofoil surface, and it is an essential parameter in determining the hydrofoil's performance. At low angles of attack, the pressure coefficient is relatively constant and close to 1, indicating that the pressure on the surface is close to the freestream pressure. As the angle of attack increases,

Citation: Farajollahi A (2023) The effect of three-type Vortex Generators (VGs) on NACA-0015 hydrofoil cavitation formation at different angles of attack. Innova Aerosp Sci Technol 1(1): 005-016. DOI: https://dx.doi.org/10.17352/iast.000002

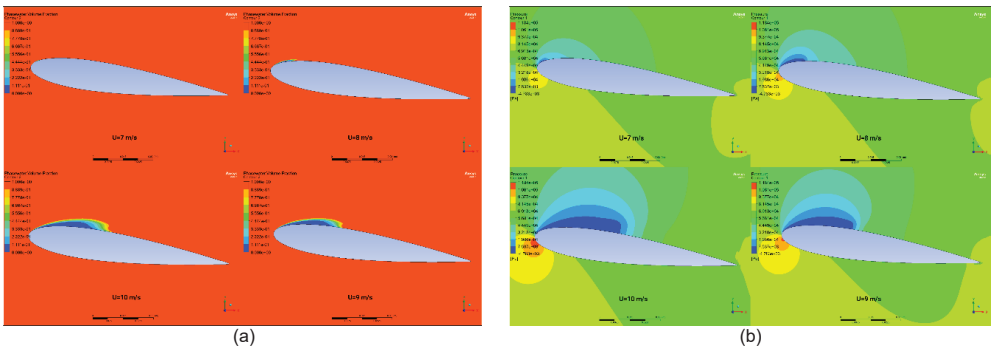

(a) (b)

Figure 7: Contours of a) Phase water volume fraction b) pressure magnitude for NACA 0015 (AoA 8).

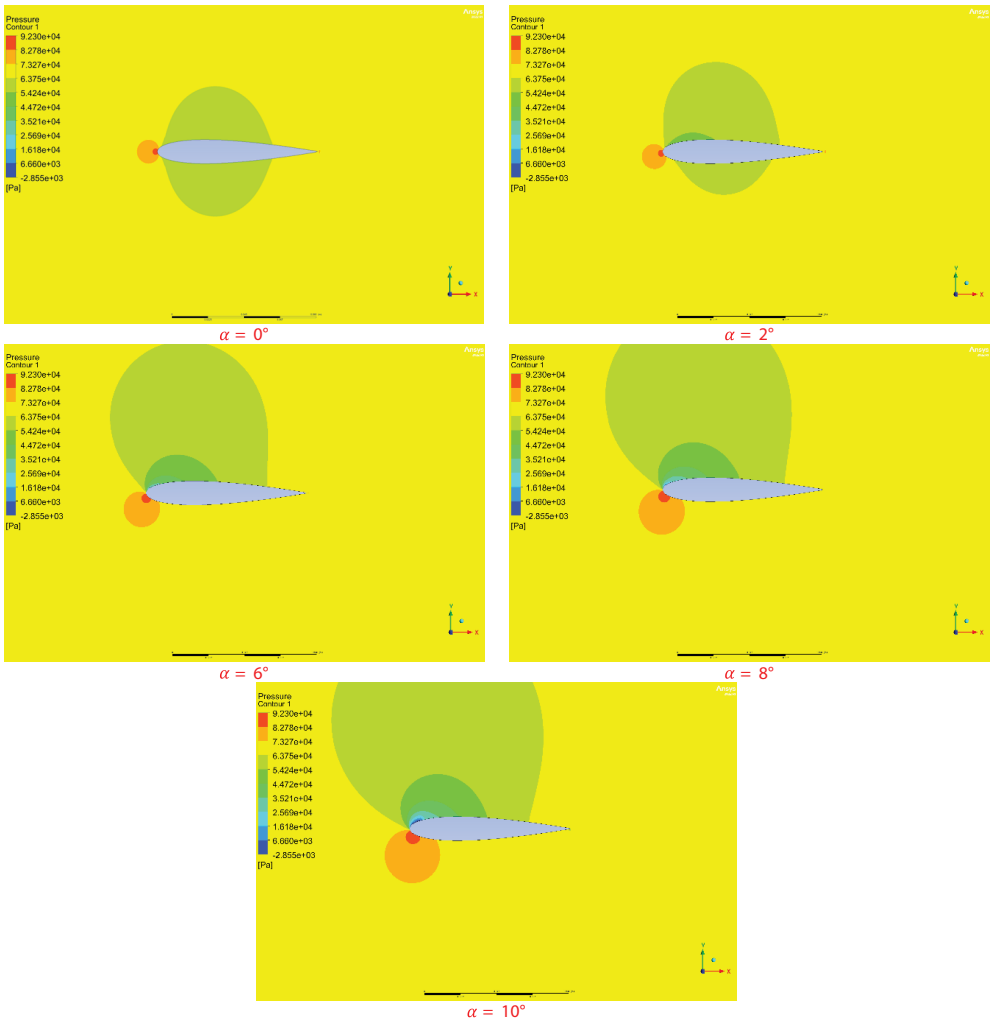

Figure 8: Comparison pairs of Static Pressure contours for NACA 0015.

the pressure on the upper surface of the hydrofoil decreases, resulting in a lower pressure coefficient. At the same time, the pressure on the lower surface increases, resulting in a higher pressure coefficient. Therefore, the pressure distribution changes with the angle of attack, and it is necessary to study the pressure coefficient to optimize the hydrofoil design (Figure 10).

The chart (Figure 11) shows the pressure coefficient (Cp) distribution on a smooth NACA0015 hydrofoil at different angles of attack (AoA). The Cp is a dimensionless quantity that is defined as the difference between the static pressure at a point on the airfoil surface and the freestream pressure divided by the freestream dynamic pressure.

The chart shows that the Cp distribution changes

Citation: Farajollahi A (2023) The effect of three-type Vortex Generators (VGs) on NACA-0015 hydrofoil cavitation formation at different angles of attack. Innova Aerosp Sci Technol 1(1): 005-016. DOI: https://dx.doi.org/10.17352/iast.000002

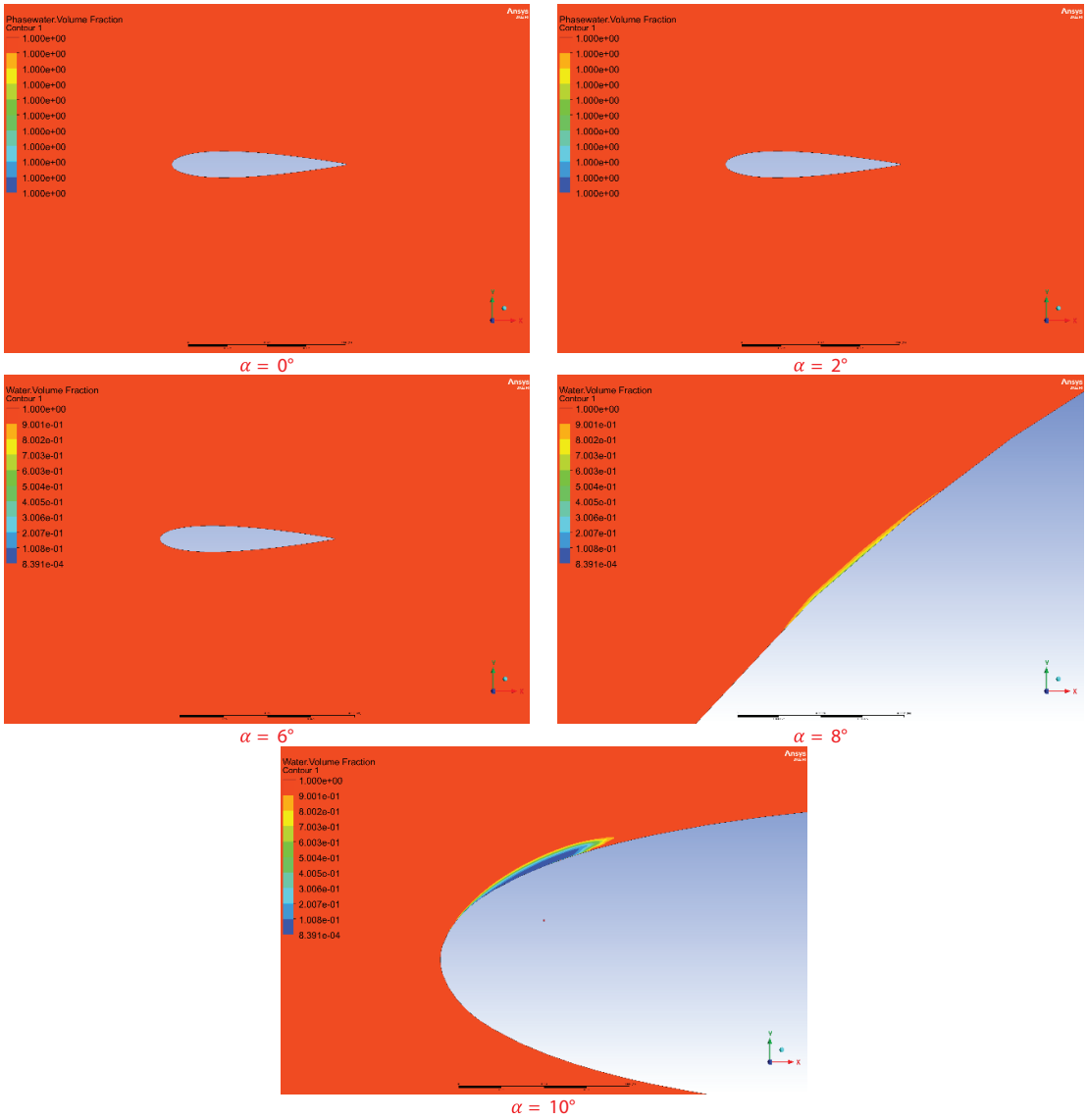

Figure 9: Comparison pairs of cavitation phenomena for NACA 0015.

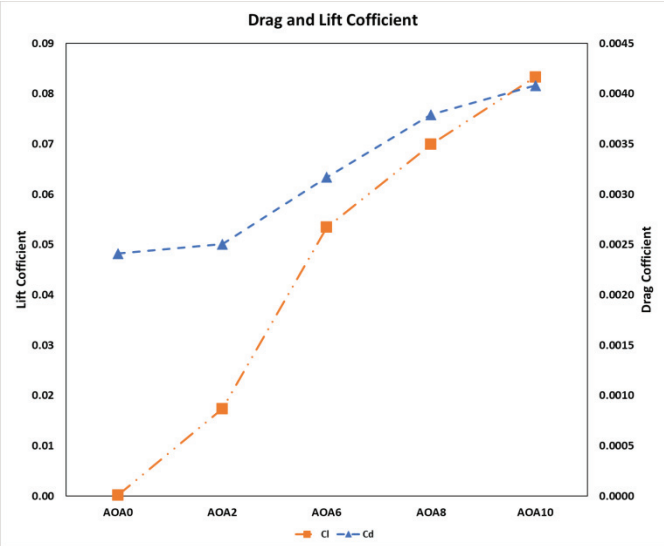

Figure 10: Comparison of Drag and Lift coefficient for different angles of attack.

significantly with AoA. For small AoA (0° and 2°), the Cp is positive on both the upper and lower surfaces of the airfoil. This indicates that the flow is attached to the airfoil, and there is no significant separation of flow over the airfoil. As the AoA increases, the Cp on the upper surface of the airfoil increases, while the Cp on the lower surface of the airfoil decreases. This indicates that the flow is becoming more attached to the upper surface of the airfoil and less attached to the lower surface of the airfoil. At AoA of 6° and 8°, the Cp on the upper surface of the airfoil reaches a maximum, and the Cp on the lower surface of the airfoil reaches a minimum. This indicates that the flow is becoming stall, and the airfoil is producing its maximum lift. At an AoA of 10°, the Cp on the upper surface of the airfoil begins to decrease, and the Cp on the lower surface of the airfoil begins to increase. This indicates that the flow is becoming detached from the airfoil, and the airfoil is producing less lift.

The chart also shows that the location of the peak and trough Cp on the airfoil surface changes with AoA. As the AoA

Citation: Farajollahi A (2023) The effect of three-type Vortex Generators (VGs) on NACA-0015 hydrofoil cavitation formation at different angles of attack. Innova Aerosp Sci Technol 1(1): 005-016. DOI: https://dx.doi.org/10.17352/iast.000002

increases, the peak Cp on the upper surface of the airfoil moves closer to the leading edge of the airfoil, and the trough Cp on the lower surface of the airfoil moves closer to the trailing edge of the airfoil. This is because the airfoil is becoming more attached to the upper surface and less attached to the lower surface as the AoA increases.

Overall, the chart shows (Figure 11) that the pressure coefficient distribution on a NACA0015 hydrofoil is characterized by a peak pressure on the upper surface of the airfoil and a trough pressure on the lower surface of the airfoil. The location of these peaks and troughs shifts with the angle of attack. The pressure coefficient distribution is also important for determining the lift and drag forces on the airfoil.

Effect of Vortex Generator (VG)

The effect of vortex generators on the pressure coefficient distribution of the NACA0015 will depend on the specific configuration of the vortex generators, including their size, shape, and location on the Hydrofoil. However, in general, the addition of vortex generators to the NACA0015 can have a positive impact on its performance.

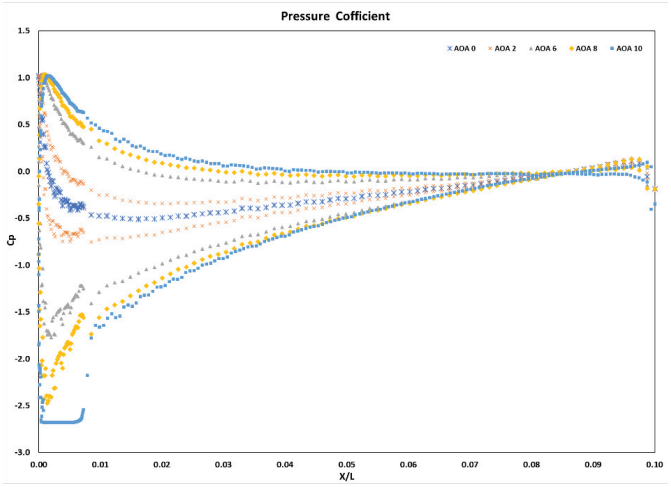

Figure 11: Pressure coefficient distribution on the smooth hydrofoil NACA0015 for different AoA (α°=0,2,6,8,10).

Table 3: Configuration of the vortex generators.

VG shape	Size[mm]	Location
Triangle	h=0.5, L=0.8	0.01C
Square	b=0.5, L=0.8	0.01C
Circle	r=0.5, D=0.8	0.01C

In this study, three types of vortex generators are considered at nearly the same size and place. The shapes are triangle, square, and circle. Table 3 and Figure 12 show the configuration of the vortex generators, including their size, shape, and location on the Hydrofoil. Boundary conditions for these three VGs are $v_{\infty} = 9\frac{m}{s}$, outlet pressure $P = 67000\ Pa$ and angle of attack 8 degrees. Simulation has been conducted in the presence of cavitation and non-cavitation models to compare the effect of VG on drag, lift, and pressure coefficient.

In terms of pressure coefficient distribution, the installation of vortex generators can lead to an increase in the pressure coefficient near the leading edge of the hydrofoil. This effect is attributed to the vortices generated by the vortex generators, which redirect the flow more effectively around the leading edge. As a result, the likelihood of separation is reduced, and the effective camber of the hydrofoil is increased. However, the use of VGs can also result in cavitation, which can cause a decrease in the pressure coefficient on the hydrofoil surface. The formation of cavitation bubbles creates small regions of low pressure, which can lower the overall pressure coefficient. As demonstrated in Figure 13, the hydrofoil with VGs exhibited a longer high-pressure coefficient. The shift in the high-pressure coefficient position varied according to the shape of the VGs. When keeping the parameters steady for all three VG shapes (Triangle, Square, and Circle), the square VG showed more high-pressure coefficient area than the other two shapes. The circle VG had a similar correlation with the square, while the triangular VG had the lowest pressure near the leading edge of the hydrofoil.

Figure 14 indicates that the pressure distribution on the lower surface of the hydrofoil remains relatively stable when the Vortex Generators (VGs) are applied. However, the application of VGs on the upper surface of the hydrofoil, specifically along its chamber line, produces significant changes in the pressure contours. These changes are particularly noticeable in the area surrounding the VGs.

The triangular shape of the VGs results in a reduction of the pressure in the border area to less than 15.4 MPa and generates

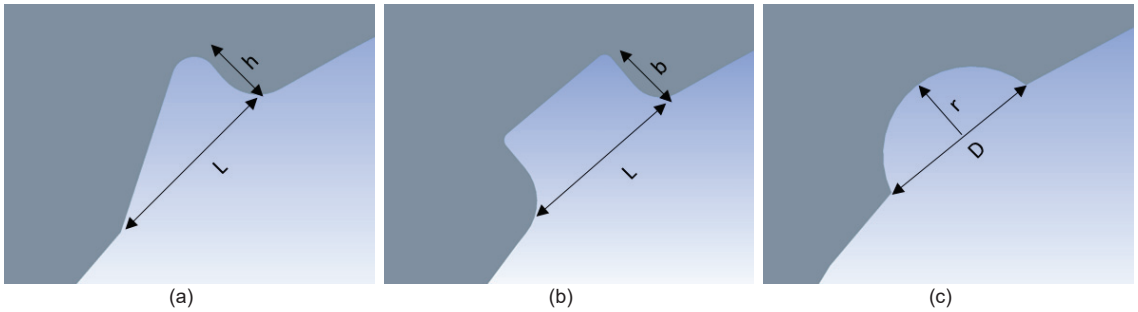

Figure 12: Vortex Generators (VGs) a) Triangle b) Square c) Circle geometry detail.

Citation: Farajollahi A (2023) The effect of three-type Vortex Generators (VGs) on NACA-0015 hydrofoil cavitation formation at different angles of attack. Innova Aerosp Sci Technol 1(1): 005-016. DOI: https://dx.doi.org/10.17352/iast.000002

cavitation at the back of the VGs. In the case of the circular and square VGs, the changes in pressure distribution are similar to each other, but the pressure distribution immediately after the VGs is somewhat irregular. The area of low pressure (less than 15.4 MPa) for the square VGs is wider than for the other shapes, but the square VGs also produce a larger cavitational region behind them (Figure 15).

Overall, the results suggest that the shape of the VGs has a significant impact on the pressure distribution and cavitation formation on the hydrofoil. These findings have important implications for the design and optimization of hydrofoils for various applications, including marine transportation and energy harvesting.

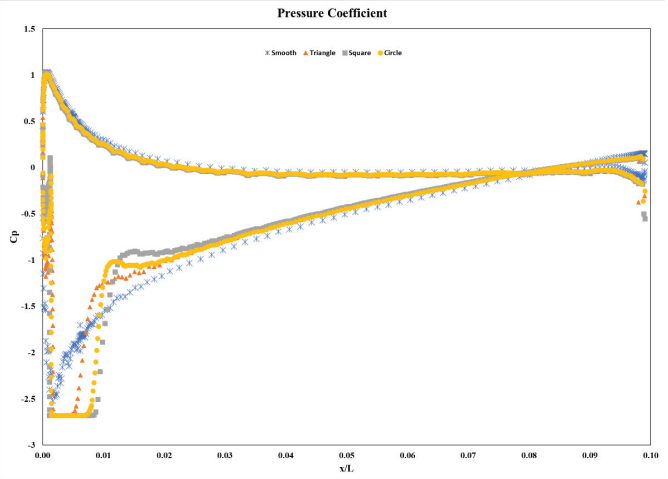

Figure 13: Pressure coefficient distribution on hydrofoil NACA0015 for different VGs.

The application of Vortex Generators (VGs) on a hydrofoil can create wake flow behind the hydrofoil. When the VGs generate vortices on the hydrofoil surface, they can induce mixing and create turbulence in the flow, which can result in a complex wake flow pattern downstream of the hydrofoil.

The wake flow created by the VGs on a hydrofoil can have both positive and negative effects on the hydrofoil's performance. On the one hand, the mixing induced by the VGs can delay flow separation and reduce drag, leading to improved hydrofoil performance. On the other hand, the wake flow can also generate turbulence and vortices that can increase drag, cause noise, and create vibration and erosion on the hydrofoil surface which happens in this case (Figure 16).

This study reports that the application of Vortex Generators (VGs) on a hydrofoil can increase its drag coefficient compared to a smooth hydrofoil. The turbulence and vortices generated by the VGs can lead to an increase in drag. Additionally, the presence of the wake flow can cause unsteady flow conditions, resulting in fluctuations in the lift generated by the hydrofoil and reducing its overall efficiency. The drag coefficient increased by more than 30%, while the decrease in the lift coefficient was less than 10% with the addition of VGs to the upper part of the hydrofoil. The square VG had the most significant increase in drag coefficient, while the circular VG had the least. The triangular VG had a drag coefficient almost equivalent to that of the square VG. The most substantial decrease in lift coefficient was observed for the square VG, while the least decrease was observed for the triangular VG. These findings are supported by Figure 16, which illustrates the drag and lift coefficients for each VG shape.

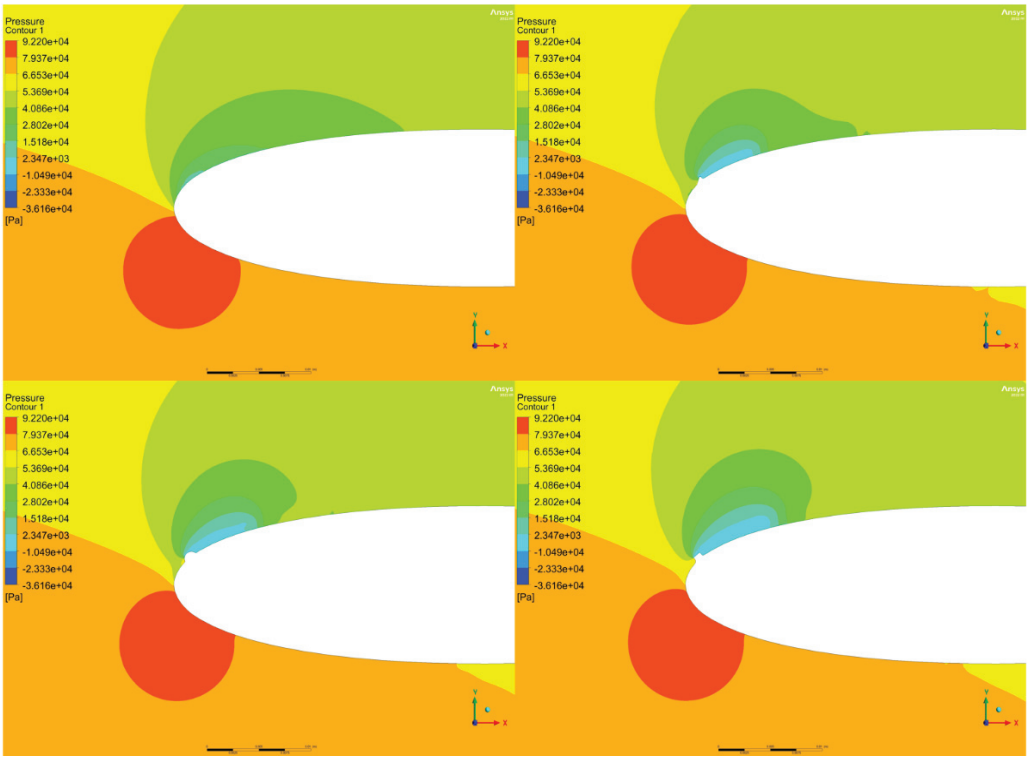

Figure 14: Pressure distribution around hydrofoil NACA0015 with and without VGs.

Citation: Farajollahi A (2023) The effect of three-type Vortex Generators (VGs) on NACA-0015 hydrofoil cavitation formation at different angles of attack. Innova Aerosp Sci Technol 1(1): 005-016. DOI: https://dx.doi.org/10.17352/iast.000002

The lift-drag ratio for smooth is more than 20 while adding VGs near to cavitation generation area leads to a decrease. Square is a structure with a lower k (lift-drag ratio) that shows a more significant impact on vortex generation and cavitation around hydrofoil (Figure 17).

Figure 17 shows the lift-drag coefficient ratio (L/D) of various vortex generators at different angles of attack (AoA). The L/D ratio is a dimensionless quantity that is defined as the ratio of the lift coefficient (Cl) to the drag coefficient (Cd). It is a measure of the aerodynamic efficiency of an airfoil or other aerodynamic body.

The chart shows that the L/D ratio of all vortex generators increases with AoA up to a certain point, and then decreases as the AoA increases further. This is because the vortex generators help to create lift at low AoA, but they also create more drag at high AoA. The peak L/D ratio of the different vortex generators varies depending on the geometry of the vortex generator. The triangle vortex generator has the highest peak L/D ratio, followed by the square vortex generator, the smooth vortex generator, and the circle vortex generator.

The chart also shows that the AoA at which the peak L/D ratio occurs is different for the different vortex generators. The triangle vortex generator has the lowest AoA at which the peak L/D ratio occurs, followed by the square vortex generator, the smooth vortex generator, and the circle vortex generator. This is because the triangle vortex generator is the most efficient at creating lift at low AoA.

In conclusion, the chart shows that vortex generators can be used to improve the L/D ratio of airfoils and other aerodynamic bodies. However, it is important to choose the right vortex generator for the application and to operate the aircraft at the correct AoA to maximize the benefit of the vortex generators.

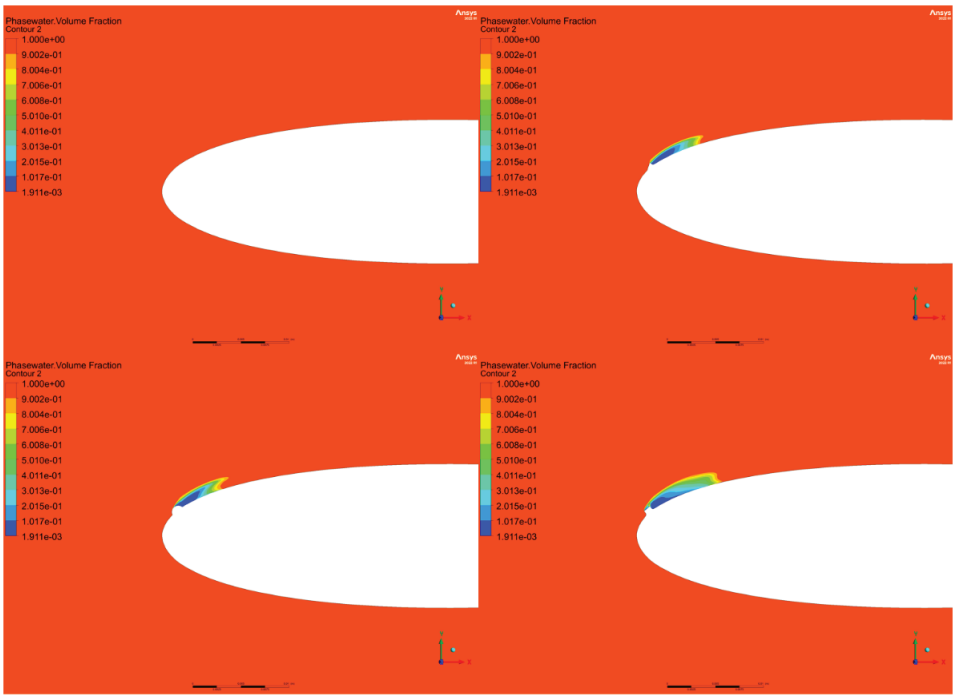

Figure 15: Contours of Phase water volume fraction for hydrofoil NACA0015 with and without VGs.

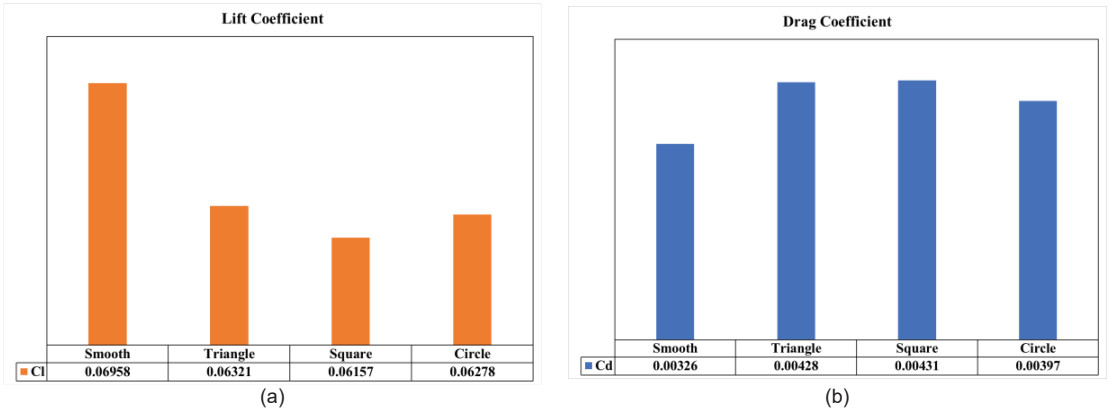

Figure 16: Effect of Vortex Generators (VGs) on hydrofoil performance a) Lift Coefficient b) Drag Coefficient.

Citation: Farajollahi A (2023) The effect of three-type Vortex Generators (VGs) on NACA-0015 hydrofoil cavitation formation at different angles of attack. Innova Aerosp Sci Technol 1(1): 005-016. DOI: https://dx.doi.org/10.17352/iast.000002

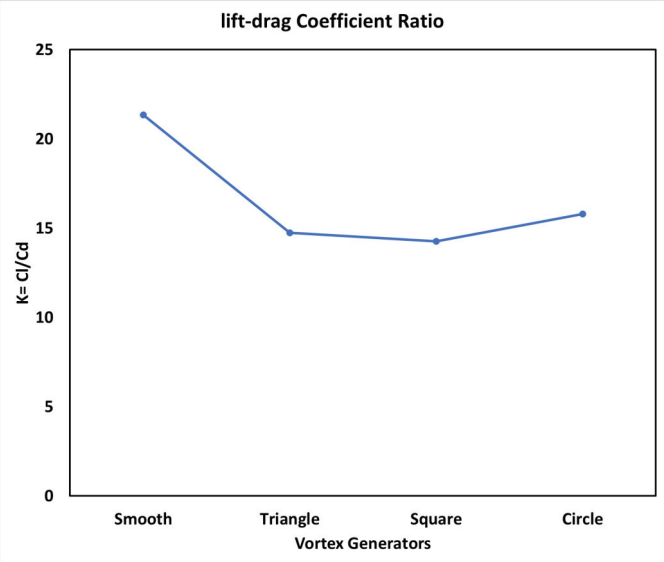

Figure 17: Lift-drag ratio for smooth and VGs hydrofoil.

Conclusion

Numerical simulations on cavitation flow around the general hydrofoil and the hydrofoil with VG on the surface were performed to investigate the effects of triangle, square, and, circle structures on the inhibition of the cavitation bubble evolution process. Also, the effect of Reynolds number on smooth hydrofoil NACA0015 and Angle of Attack (AoA) variation has been mentioned.

1. Reynolds number effect can be seen on NACA0015 AoA 8 with an increase of drag coefficient and reverse trend for lift coefficient in a specific range of Reynolds number. Pressure distribution around the hydrofoil is changed by velocity increase that caused a wider low-pressure area near the leading edge of the hydrofoil and more cavitation bubble evaluation.

2. The effect of Angle of Attack (AoA) in the range of 0 to 10 showed an increase in drag and lift coefficient simultaneously while the study showed that AoA over an 8-degree lift-drag ratio gradually gets less change in comparison to beginning AoA (1-6). At low angles of attack, the pressure coefficient is close to 1, indicating that ýthe pressure on the surface is close to the freestream pressure. As the angle of attack increases, the ýpressure on the upper surface of the hydrofoil decreases, resulting in a lower pressure coefficient. At ýthe same time, the pressure on the lower surface increases, resulting in a higher pressure coefficient.

3. According to a study, the use of Vortex Generators (VGs) on a hydrofoil can result in an increase in its drag coefficient when compared to a hydrofoil without VGs. This is due to the turbulence and vortices that are created by the VGs, which can cause an increase in drag. Furthermore, the presence of wake flow can lead to unsteady flow conditions, resulting in fluctuations in the lift produced by the hydrofoil and a decrease in its overall efficiency.

4. In terms of drag coefficient, the square VG generated the highest increase, while the circular VG showed the least increase. The triangular VG produced a drag coefficient that was almost equal to that of the square VG. Regarding the decrease in lift coefficient, the square VG had the most significant reduction, while the triangular VG had the least.

References

1. Franc JP, Michel JM. Attached cavitation and the boundary layer: experimental investigation and numerical treatment. Journal of Fluid Mechanics. 1985; 154: 63-90.

2. Kjeldsen M, Arndt REA, Effertz M.Spectral Characteristics of Sheet/Cloud Cavitation. Journal of Fluids Engineering. 2000; 122(3): 481-487.

3. Adama Maiga M, Coutier-Delgosha O, Buisine D. A new cavitation model based on bubble-bubble interactions. Physics of Fluids. 2018; 30(12).

4. Kannan YS, Karri B, Sahu KC. Letter: Entrapment and interaction of an air bubble with an oscillating cavitation bubble. Physics of Fluids. 2018; 30(4).

5. Chen L. Influence of water quality on the tip vortex cavitation inception. Physics of Fluids. 2019; 31(2).

6. Foeth EJ, van Terwisga T, van Doorne C. On the Collapse Structure of an Attached Cavity on a Three-Dimensional Hydrofoil. Journal of Fluids Engineering. 2008; 130(7).

7. Teran LA. Interaction of particles with a cavitation bubble near a solid wall. Physics of Fluids. 2018; 30(12).

8. Leger AT, Ceccio SL. Examination of the flow near the leading edge of attached cavitation. Part 1. Detachment of two-dimensional and axisymmetric cavities. Journal of Fluid Mechanics. 1998; 376: 61-90.

9. Leger AT, Bernal LP, Ceccio SL. Examination of the flow near the leading edge of attached cavitation. Part 2. Incipient breakdown of two-dimensional and axisymmetric cavities. Journal of Fluid Mechanics. 1998; 376: 91-113.

10. Arakeri VH, Acosta AJ. Viscous Effects in the Inception of Cavitation on Axisymmetric Bodies. Journal of Fluids Engineering. 1973; 95(4): 519-527.

11. Rood EP. Review—Mechanisms of Cavitation Inception. Journal of Fluids Engineering. 1991; 113(2): 163-175.

12. Churkin SA. Cavitation on NACA0015 hydrofoils with different wall roughness: high-speed visualization of the surface texture effects. Journal of Visualization. 2016; 19(4): 587-590.

13. Ezzatneshan E. Study of surface wettability effect on cavitation inception by implementation of the lattice Boltzmann method. Physics of Fluids. 2017; 29(11).

14. Arakeri VH. Viscous effects on the position of cavitation separation from smooth bodies. Journal of Fluid Mechanics. 1975; 68(4): 779-799.

15. Goto A, Zangeneh M. Hydrodynamic Design of Pump Diffuser Using Inverse Design Method and CFD. Journal of Fluids Engineering. 2002; 124(2): 319-328.

16. Zangeneh M. A compressible three-dimensional design method for radial and mixed flow turbomachinery blades. International Journal for Numerical Methods in Fluids. 1991; 13(5): 599-624.

17. Zhu B, Chen H. Analysis of the Staggered and Fixed Cavitation Phenomenon Observed in Centrifugal Pumps Employing a Gap Drainage Impeller. Journal of Fluids Engineering. 2017; 139(3).

Citation: Farajollahi A (2023) The effect of three-type Vortex Generators (VGs) on NACA-0015 hydrofoil cavitation formation at different angles of attack. Innova Aerosp Sci Technol 1(1): 005-016. DOI: https://dx.doi.org/10.17352/iast.000002

18. Kato H. Suppression of Sheet Cavitation Inception by Water Discharge through Slit. Journal of Fluids Engineering. 1987; 109(1): 70-74.

19. Jin W. Cavitation generation and inhibition. I. Dominant mechanism of turbulent kinetic energy for cavitation evolution. AIP Advances. 2021; 11(6).

20. Shi W. Cavitation observations and noise measurements of horizontal axis tidal turbines with biomimetic blade leading-edge designs. Ocean Engineering. 2016; 121: 143-155.

21. Lu F. Application of the vortex generator to control the PHV cavitation. Journal of Ship Mechanics. 2009; 13(6): 873-879.

22. Sun T. Evaluation of effect of micro-vortex generator on dynamic characteristics of unsteady partial cavitating flow over hydrofoil. Ocean Engineering. 2022; 257: 111601.

23. Lu F. Application of the vortex generator to control the PHV cavitation. 2009; 13: 873-879.

24. Kadivar E. An experimental investigation of transient cavitation control on a hydrofoil using hemispherical vortex generators. Journal of Hydrodynamics. 2021; 33(6): 1139-1147.

25. Qiu N. Effects of microvortex generators on cavitation erosion by changing periodic shedding into new structures. Physics of Fluids. 2020; 32(10).

26. Che B. Control effect of micro vortex generators on leading edge of attached cavitation. Physics of Fluids. 2019; 31(4).

Citation: Farajollahi A (2023) The effect of three-type Vortex Generators (VGs) on NACA-0015 hydrofoil cavitation formation at different angles of attack. Innova Aerosp Sci Technol 1(1): 005-016. DOI: https://dx.doi.org/10.17352/iast.000002